Simultaneous Binding of Ruthenium(II) [(1,10-Phenanthroline)$_2$dipyridophenazine]$^{2+}$ and Minor Groove Binder 4′,6-Diamidino-2-phenylindole to Poly[d(A−T)$_2$] at High Binding Densities: Observation of Fluorescence Resonance Energy Trasfer Across the DNA Stem

Byeong Hwa Yun,[†] Jin-Ok Kim,[†] Bae Wook Lee,[†] Per Lincoln,[‡] Bengt Nordén,[‡] Jong-Moon Kim,[§] and Seog K. Kim*,[†]

Department of Chemistry, College of Sciences, Youngnam University, Dae-dong, Kyoungsan City, Kyoung-buk, 712-749 Republic of Korea, Department of Physical Chemistry, Chalmers University of Technology, S 412 96 Gothenburg, Sweden, and Division of Life and Molecular Sciences, Pohang University of Science and Technology, San 31, Hyoja-dong, Nam-gu, Pohang, Kyungbuk, 790-784 Republic of Korea

Received: December 26, 2002; In Final Form: May 23, 2003

Photophysical properties of Δ- and Λ-[Ru(phenanthroline)$_2$dipyrido[3,2-*a*:2′,3′-*c*]phenazine]$^{2+}$ ([Ru(phen)$_2$DPPZ]$^{2+}$) bound to poly[d(A−T)$_2$] in the presence and absence of 4′,6-diamidino-2-phenylindole (DAPI) has been studied. In the presence of DAPI, the minor groove of poly[d(A−T)$_2$] is blocked, allowing comparison of the binding mode of the ruthenium complexes. Absorption and circular dichroism (CD) as well as flow linear dichroism (LD) of the Λ-enantiomer are essentially unaffected when the minor groove is blocked by DAPI or not. However, with the Δ-enantiomer LD suggests a small but distinct change in binding geometry for both the DAPI and the ruthenium complex when DAPI is simultaneously bound to poly[d(A−T)$_2$]. In all cases, the DPPZ ligand of the metal complex is intercalated between the nucleobases. From these data, it is concluded that the ruthenium complex still binds to DNA with the Ru(phen)$_2$ moiety of both the Λ- and Δ-enantiomer located in the major groove when the minor groove is blocked. When DAPI and the ruthenium complex ions are simultaneously bound to poly[d(A−T)$_2$], the luminescence of DAPI is decreased and that of the ruthenium complex is increased. The intensity ratio of the excitation relative to absorption spectra of the ruthenium complex is similar to the absorption spectrum of DAPI, demonstrating that excitation energy of DAPI is transferred to the ruthenium complex across the stem of DNA.

Introduction

The interactions of DNA with transition metal complexes containing planar polycyclic heteroaromatic ligands have been widely studied.[1] In particular, derivatives of the chiral [Ru(phen)$_3$]$^{2+}$ (phen = 1,10-phenanthroline) complex have been investigated as probes of nucleic acids structure,[2−6] as artificial photonucleases,[7−9] as fluorescent hybridization probes,[10−14] and in electron-transfer systems.[15−25] Although the exact binding mode to DNA of the parent [Ru(phen)$_3$]$^{2+}$ complex has been a controversial issue,[3,26−33] when one phenanthroline is replaced by a larger ligand, e.g., DPPZ (dipyrido[3,2-*a*:2′,3′-*c*]phenazine, Figure 1) or BDPPZ (benzodipyrido[*b*:3,2-*h*:2′,3′-*j*]phenazine), the extended ligand is undoubtedly classically intercalated between DNA base pairs.[12,34−41] However, whether the metal complex intercalates from the major groove or from the minor groove has also been a matter of debate. Whereas ^{1}H NMR NOE data suggest that both enantiomers of [Ru(phen)$_3$]$^{2+}$ interact with the minor groove of short oligomer duplexes, intercalation from the major groove was inferred for [Ru(phen)$_2$DPPZ]$^{2+}$.[36] On the other hand, spectral properties, including absorption, circular dichroism (CD), and linear dichroism (LD) of [Ru(phen)$_2$DPPZ]$^{2+}$ bound to poly(dA)·[poly(dT)]$_2$ triplex, in which the major groove of the template poly(dA)·poly(dT) duplex is blocked by the Hoogsteen paired third poly(dT) strand, remained to the same as those bound to the poly(dA)·poly(dT) duplex, supporting intercalation of the extended ligand from the minor groove.[39] A spectroscopic study with T4 DNA, which is glycosylated in the major groove, has also suggested that the ruthenium complexes bind from the minor groove,[40] as have several recent ^{1}H NMR studies.[41,42] However, addition of a minor groove binding drug, distamycin, to the *rac*-[Ru(phen)$_2$DPPZ]$^{2+}$−poly[d(A−T)$_2$] complex resulted in an

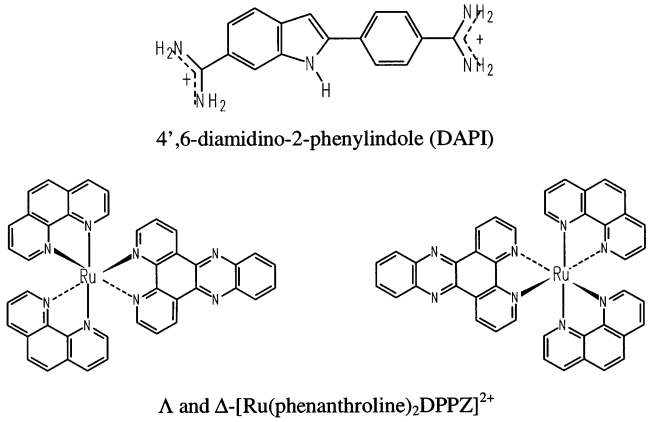

Figure 1. Structures of 4′,6-diamidino-2-phenylindole (DAPI) and Δ- and Λ-enantiomers of [Ru(phenanthroline)$_2$dipyrido[3,2-*a*:2′,3′-*c*]phenazine]$^{2+}$ ([Ru(phen)$_2$DPPZ]$^{2+}$).

* To whom correspondence should be addressed. Tel: 82 53 810 2362. Fax: 82 53 815 5412. E-mail: seogkim@yu.ac.kr.
† Youngnam University.
‡ Chalmers University of Technology.
§ Pohang University of Science and Technology.

10.1021/jp027828n CCC: $25.00
Published on Web 08/16/2003

increase in ruthenium emission up to a 1:5 distamycin/DNA base pair ratio whereas, in contrast, the addition of the major-groove intercalator Δ,α-[Rh[(*R*,*R*)-Me_2trien]phi]$^{3+}$ to the *rac*-[Ru(phen)$_2$DPPZ]$^{2+}$−[d(5′-GAGTGCACTC-3′)$_2$] complex decreased the emission yield of the ruthenium complex. Both of these observations are consistent with the intercalation of ruthenium complexes from the major groove.[43]

In this study, CD and LD spectral properties of the enantiomers of [Ru(phen)$_2$DPPZ]$^{2+}$ bound to poly[d(A−T)$_2$] in the presence or absence of an established minor groove binding drug, 4′,6-diamidino-2-phenylindole (DAPI, Figure 1),[44,45] are compared. During the course of this work, we have further observed a strong attenuation of the luminescence emission intensity of the DAPI molecule and a corresponding enhancement of [Ru(phen)$_2$DPPZ]$^{2+}$ when these chromophores are simultaneously bound to DNA, suggesting the excitation energy of DAPI is transferred to the metal complex across the DNA stem.

Experiment

Materials. Pure [Ru(phen)$_2$DPPZ]$^{2+}$ enantiomers were prepared as reported previously and the concentration was determined using an extinction coefficient of 20 000 M^{-1} cm^{-1} at 439 nm.[35] DAPI was purchased from Sigma and used without further purification; the extinction coefficient of DAPI is 27 000 M^{-1} cm^{-1} at 342 nm. Poly[d(A−T)$_2$] purchased from Pharmacia was dissolved in 5 mM cacodylate buffer (pH 7.0) containing 100 mM NaCl and 1 mM EDTA, followed by several times of dialysis against 5 mM cacodylate buffer (pH 7.0). This buffer is used throughout this work. Poly[d(A−T)$_2$] concentration was determined using an extinction coefficient of 6600 M^{-1} cm^{-1} per nucleotide base at 262 nm.

CD and LD Spectrum. Measurement and data analysis of CD and LD of the drug−DNA complexes have been described previously.[46−48] CD spectra for the [Ru(phen)$_2$DPPZ]$^{2+}$−DAPI−poly[d(A−T)$_2$] system were recorded on a JASCO-J715 spectropolarimeter. The LD spectrum, which is defined as the differential absorption spectrum of light polarized parallel and perpendicular to a laboratory reference axis, was measured on a JASCO-J720 spectropolarimeter on flow oriented DNA samples in a Couette cell device as described by Nordén and Seth.[48] Qualitatively, a positive LD signal in the drug absorption region excludes the possibility of drug intercalation whereas a negative, large LD signal is indicative of intercalation.[46,47]

Absorption Spectrum and Fluorescence Quenching. Fluorescence intensities were measured on a JASCO FP-777 spectrofluorometer. In the course of titration, small aliquots of the titrant were added to the sample solution and volume corrections were made. The emission intensities of DAPI were monitored through the excitation and emission at 360 and 450 nm, respectively. At these wavelengths, changes in DAPI fluorescence can be monitored without interference with the ruthenium fluorescence. Fluorescence changes of the ruthenium complex were followed through 439 and 610 nm for excitation and emission, respectively. Absorption spectra were recorded on a Hewlett-Packard 8452A diode array or a JASCO V-550 spectrophotometer.

Energy Transfer. The concept of fluorescence resonance energy transfer, originally reported by Le Peq and Paoletti,[49] for transfer from DNA bases to intercalated ethidium, has been used occasionally as an indicator for a drug being intercalated between, or in contact with, the DNA bases.[37,50,51] Similarly, the energy transfer from DAPI to [Ru(phen)$_2$DPPZ]$^{2+}$ in the [Ru(phen)$_2$DPPZ]$^{2+}$−poly[d(A−T)$_2$]−DAPI complex could be analyzed by plotting the ratio of quantum efficiencies $Q(\lambda)$ of the [Ru(phen)$_2$DPPZ]$^{2+}$ in the presence and absence of DAPI in the DAPI absorption region (300−400 nm):

$$Q(\lambda) = \frac{I_p(\lambda)\, A_a(\lambda)}{I_a(\lambda)\, A_p(\lambda)}$$

where $I_p(\lambda)$ is the luminescence spectrum of the DNA-bound metal complex in the presence of DAPI and $I_a(\lambda)$ is the intensity in the absence of DAPI; $A_a(\lambda)$ and $A_p(\lambda)$ are the corresponding absorption spectra.

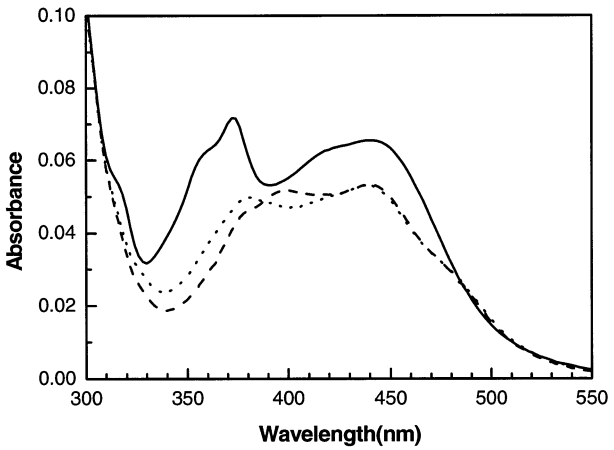

Figure 2. Absorption spectra of the Δ-[Ru(phen)$_2$DPPZ]$^{2+}$ complex in the absence of DNA (solid curve), in the presence of poly[d(A−T)$_2$] (dotted curve), and in the presence of DAPI−poly[d(A−T)$_2$] (dashed curve). The dashed curve was produced by the subtraction of the absorbance spectrum of DAPI−poly[d(A−T)$_2$] from that of the Δ-[Ru(phen)$_2$DPPZ]$^{2+}$−poly[d(A−T)$_2$]−DAPI sample to facilitate comparison. [DAPI] = 3 μM, [polynucleotide] = 30 μM nucleobase and [ruthenium complex] = 2.4 μM.

Results

Absorption and Circular Dichroism. Absorbance spectra of the [Ru(phen)$_2$DPPZ]$^{2+}$ bound to duplex poly[d(A−T)$_2$] and DAPI−poly[d(A−T)$_2$] complex, respectively, as well as for free [Ru(phen)$_2$DPPZ]$^{2+}$ complex, are shown in Figure 2. The absorption spectra of appropriate duplex poly[d(A−T)$_2$] and DAPI−poly[d(A−T)$_2$] samples are subtracted from those of the mixtures. The spectra of the Λ- and Δ-enantiomers are within experimental error the same, so only that of the Δ-enantiomer is shown. The ruthenium complex exhibits hypochromism and red shift throughout the entire absorption region upon binding to duplex poly[d(A−T)$_2$] as well as to DAPI−poly[d(A−T)$_2$]. Hypochromism and red shift indicate strong interactions between the DNA bases and the DPPZ ligand, which is consistent with an intercalation geometry for this extended ligand. The extent of hypochromism and red shift is particularly pronounced in the intraligand absorption region (∼370 nm) for the ruthenium complex upon binding to the duplex poly[d(A−T)$_2$] and to the DAPI−poly[d(A−T)$_2$] complex, suggesting the interaction between the DNA bases and the extended DPPZ ligand is similar whether DAPI is present in the minor groove or not.

CD spectra of Δ- and Λ-[Ru(phen)$_2$DPPZ]$^{2+}$ at various concentrations in the presence of the DAPI−poly[d(A−T)$_2$] complex are shown in Figure 3a,b. When DAPI is bound to the minor groove of poly[d(A−T)$_2$], it exhibits a positive strong induced CD signal in the 300−400 nm region.[44] We observed a similar positive CD signal for the DAPI−poly[d(A−T)$_2$] complex (Figure 3a,b, insets). This positive CD signal remained unchanged also in the presence of the ruthenium complexes,

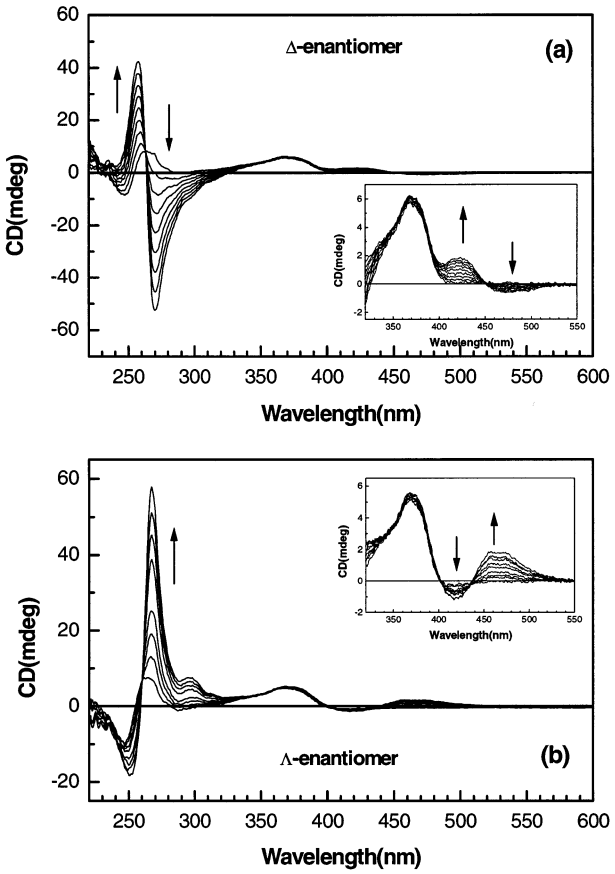

Figure 3. CD spectra of (a) Δ-$[Ru(phen)_2DPPZ]^{2+}$ and (b) Λ-$[Ru(phen)_2DPPZ]^{2+}$ complexes in the presence of DAPI−poly[d(A−T)$_2$]. [DAPI] = 3 μM, [polynucleotide] = 30 μM in nucleobase. The concentrations of ruthenium complex were 0.0, 0.3, 0.6, 0.9, 1.2, 1.5, 1.8, 2.1, and 2.4 μM, increasing in the direction of the arrow.

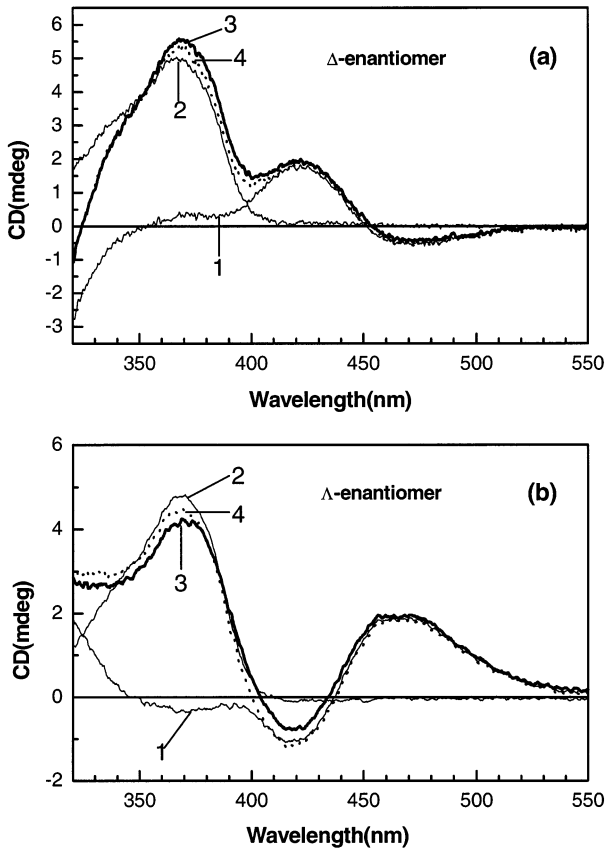

Figure 4. CD spectra of the $[Ru(phen)_2DPPZ]^{2+}$ (curve 1) and DAPI (curve 2) bound to poly[d(A−T)$_2$], sum of curves 1 and 2 (dotted curve; curve 4) and CD spectrum of the $[Ru(phen)_2DPPZ]^{2+}$−poly[d(A−T)$_2$]−DAPI complex (thick solid curve; curve 3). [DAPI] = 3 μM, [polynucleotide] = 30 μM nucleobase, [ruthenium complex] = 2.4 μM. (a) Δ- and (b) Λ-enantiomer.

indicating that the binding of the metal complexes does not result in any significant release or displacement of DAPI molecules. Several isosbestic points (262 and 450 nm for the Δ-enantiomer and 260 and 434 nm for the Λ-enantiomer) indicates a homogeneous binding mode for both metal complexes in the presence of DAPI.

Analysis of the CD spectrum of the $[Ru(phen)_2DPPZ]^{2+}$−DAPI−poly[d(A−T)$_2$] complex in the DNA absorption region (below 320 nm) is complicated because of several potential contributions to CD, including induced CD and possible conformational change of DNA as a result of the drug binding. CD spectra of DAPI−poly[d(A−T)$_2$], Δ-$[Ru(phen)_2DPPZ]^{2+}$−poly[d(A−T)$_2$], and Δ-$[Ru(phen)_2DPPZ]^{2+}$−DAPI−poly[d(A−T)$_2$] complexes in the long wavelength region (above 320 nm, where DNA does not contribute) are compared in Figure 4a. The CD spectrum for the Λ-enantiomer system is shown in Figure 4B. For each enantiomer, the CD spectrum of $[Ru(phen)_2DPPZ]^{2+}$−DAPI−poly[d(A−T)$_2$] is particularly identical to the sum of the respective CD spectra of the $[Ru(phen)_2DPPZ]^{2+}$−poly[d(A−T)$_2$] and DAPI−poly[d(A−T)$_2$] samples, showing that no major conformation change occurs, neither for DAPI nor for the metal complex bound to poly[d(A−T)$_2$], and that no significant release or displacement of bound drug occurs as a result of the simultaneous presence of the two drugs at high drug to DNA ratios (see legend of Figure 4 for [drug]/[DNA] ratios).

Linear Dichroism. Flow LD was measured for various concentrations of the ruthenium complex in the presence of 100 μM poly[d(A−T)$_2$] and 25 μM DAPI, i.e., under conditions where the minor groove should be saturated with DAPI. The resulting LD spectra are shown in Figure 5a (Δ-enantiomer) and Figure 5b (Λ-enantiomer). For both complexes, isosbestic points observed at 287, 408, and 456 nm for Δ, and at 273, 396, and 456 nm for Λ, indicate that the binding mode of the metal complexes to the DAPI−poly[d(A−T)$_2$] complex is homogeneous. In contrast to the case of CD, the LD spectra in the visible region are not identical simply to the sum of the corresponding $[Ru(phen)_2DPPZ]^{2+}$−poly[d(A−T)$_2$] and DAPI−poly[d(A−T)$_2$] spectra, but the positive LD band of DAPI at 350 nm decreases. This effect, which is more pronounced for the Δ-enantiomer than for the Λ form, is, at least partly, explained by the observation that the magnitude of the LD in the UV region (dominated by the nucleobase contribution) decreases by about 30% when the Δ-enantiomer is added (Figure 5a) compared to about 10% for Λ-enantiomer (Figure 5b), which indicates that the ability of orientation of the DNA decreases upon addition of the Δ-enantiomer, as has been previously observed.[35,38] To compensate for this orientation change, and to find out if the shape of the LD spectrum of the metal complex has changed, a DAPI−poly[d(A−T)$_2$] LD spectrum, appropriately scaled to match the orientation change, was subtracted from the final spectrum of the titration (with 10 μM $[Ru(phen)_2DPPZ]^{2+}$). In this way a spectral profile that is very similar to the profile in the absence of DAPI was obtained for the Λ-enantiomer, whereas surprisingly, for the Δ-enantiomer, the LD spectrum is clearly distinct from the one in the absence of DAPI (Figure 6) and rather resembles the LD profile of the pure Λ-enantiomer.

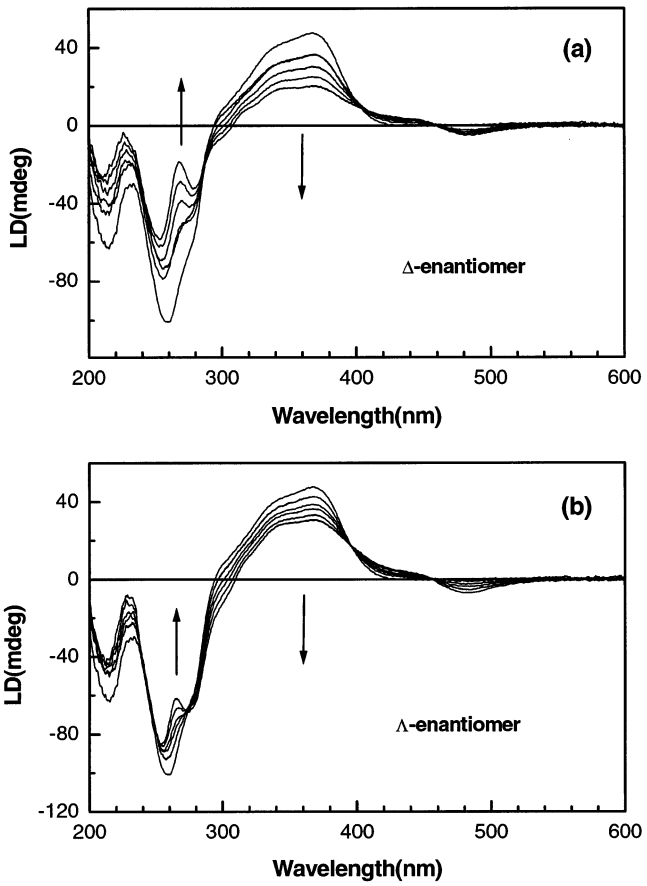

Figure 5. LD spectra of Δ- (a) and Λ- (b) $[Ru(phen)_2DPPZ]^{2+}$ bound to the DAPI−poly[d(A−T)$_2$] complex. [DAPI] = 25 μM, [polynucleotide] = 100 μM in nucleobase. The concentrations of the $[Ru(phen)_2DPPZ]^{2+}$ were 0, 2, 4, 6, 8, and 10 μM in order of arrow direction.

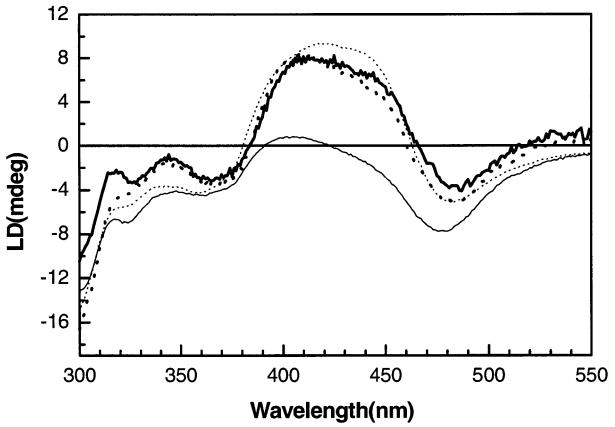

Figure 6. Linear combinations of LD spectra of Figure 5a,b. The solid curve and dotted curve denote appropriately scaled LD spectra of, respectively, Δ- and Λ-$[Ru(phen)_2DPPZ]^{2+}$ bound to calf thymus DNA. The thick solid curve denotes Δ-$[Ru(phen)_2DPPZ]^{2+}$−poly[d(A−T)$_2$]−DAPI complex, and the dashed curve, Λ-enantiomer. Conditions: 25 μM DAPI, 100 μM poly[d(A−T)$_2$], and 10 μM Δ- or Λ-$[Ru(phen)_2DPPZ]^{2+}$. Curves were produced as described in text.

Fluorescence Measurements. The change in the fluorescence intensity of DAPI−poly[d(A−T)$_2$] upon increasing ruthenium complex concentration is depicted in Figure 7a. A sample containing 30 μM poly[d(A−T)$_2$] and 3 μM DAPI was titrated by either Δ- or Λ-$[Ru(phen)_2DPPZ]^{2+}$; with DAPI occupying five base pairs of the minor groove of poly[d(A−T)$_2$], this condition may correspond to the minor groove of the poly[d(A−T)$_2$] being saturated.[44] The fluorescence intensity of the DAPI−

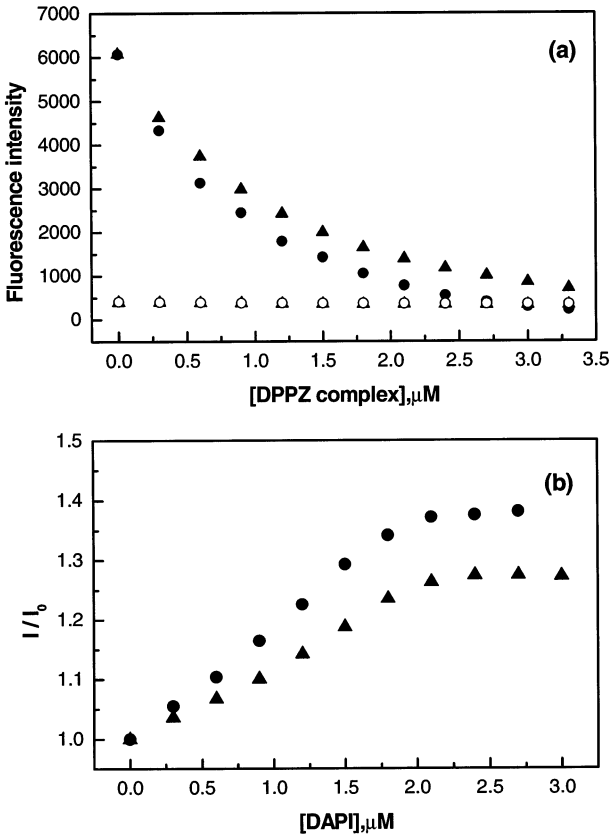

Figure 7. (a) Fluorescence intensity of DAPI bound to poly[d(A−T)$_2$] as a function of concentration of ruthenium complex: (circles) Λ-enantiomer; (triangles) Δ-enantiomer; (open symbols) the same metal complexes in the absence of poly[d(A−T)$_2$]. Excitation and emission wavelengths were 360 and 450 nm, respectively. Slit widths were 3 nm. [DAPI] = 3 μM, [polynucleotide] = 30 μM in nucleobase. (b) Increase in fluorescence intensity of $[Ru(phen)_2DPPZ]^{2+}$−poly[d(A−T)$_2$] with increasing DAPI concentration. I_o and I denote the fluorescence intensity of the metal complex in the absence and presence of DAPI, respectively. [Ruthenium complex] = 3 μM, [polynucleotide] = 30 μM. Excitation and emission wavelengths were 439 and 610 nm, respectively, and slit widths 5 nm. Key: (circles) Λ-enantiomer; (triangles) Δ-enantiomer.

poly[d(A−T)$_2$] decreased with increasing concentration of ruthenium complex. The decrease is, however, considerably more efficient for the Λ-enantiomer compared to the Δ-enantiomer. Note that with poly[d(A−T)$_2$] absent, quenching of DAPI fluorescence by the metal complex is negligible (Figure 7a), ensuring that the simultaneous assembly of DAPI and ruthenium complex on DNA is necessary for energy transfer. It was also ensured that the fluorescence of the metal complex at appropriate excitation and emission wavelengths (360 and 450 nm, respectively) was negligible (data not shown) and, thus, that the emission decrease is entirely from the DAPI molecule. The luminescence intensity of both Δ- and Λ-$[Ru(phen)_2DPPZ]^{2+}$ complexes bound to poly[d(A−T)$_2$] (excitation at 439 nm, emission at 610 nm, where DAPI does not fluoresce) increased with increasing DAPI concentration (Figure 7b). These increases were accompanied by decreasing DAPI fluorescence and the maximum fluorescence was observed with a DAPI concentration of 2.5 μM, which corresponds to a stoichiometry of six base pairs per each DAPI molecule. Again, the increase in emission intensity was more pronounced for the Λ-compared to the Δ-enantiomer.

Energy Transfer from DAPI to Ruthenium Chromophore. The $[Ru(phen)_2DPPZ]^{2+}$ complex, which is nonluminescent in aqueous solution, becomes brightly luminescent upon binding

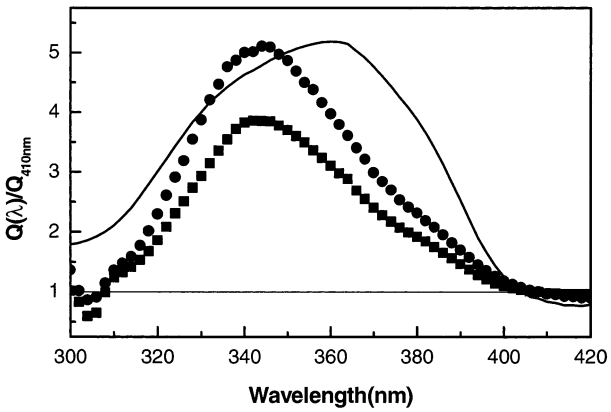

Figure 8. Excitation intensity ratio, $Q(\lambda)/Q_{410nm}$, for Δ-[Ru(phen)$_2$DPPZ]$^{2+}$ (squares) and Λ-[Ru(phen)$_2$DPPZ]$^{2+}$ (circles) bound to DAPI−poly[d(A−T)$_2$]. The excitation spectrum was recorded through 610 nm emission. Slit widths were 5 nm for both emission and excitation. The absorption spectrum of DAPI bound to poly[d(A−T)$_2$] is also shown as a solid curve for comparison.

to DNA. The change in luminescence intensity is thought to be the decrease of water activity around the metal complex at the binding site. An additional increase in emission intensity of the ruthenium complexes was observed in the presence of DAPI (Figure 7b). As an attempt to find out the additional source of the emission increase, the efficiency of energy transfer from DAPI to the metal complexes was studied (see Experimental Section). When the ratio$\{Q(\lambda)\}/\{Q_{410nm}\}$of the [Ru(phen)$_2$DPPZ]$^{2+}$−poly[d(A−T)$_2$] to the [Ru(phen)$_2$DPPZ]$^{2+}$−poly[d(A−T)$_2$]−DAPI complexes was plotted as a function of wavelength, the shapes of the resulting curves are similar to the DAPI absorption spectrum, indicating that significant energy transfer occurs from DAPI to the metal complex chromophore (Figure 8). It is also noticeable that the ratio $\{Q(\lambda)\}/\{Q_{410nm}\}$is significantly higher for the Λ-enantiomer compared to the Δ-enantiomer, which again reflects the fact that the quenching of DAPI fluorescence by the Λ-enantiomer is more effective than by the Δ-enantiomer.

Discussion

DNA Binding Modes of DAPI and [Ru(phen)$_2$DPPZ]$^{2+}$. The analysis of absorption and CD spectra show that both metal complex and DAPI can bind simultaneously to poly[d(A−T)$_2$] also at high binding densities. The CD titrations show that the CD of both the ruthenium and DAPI chromophores are unchanged even at the highest total mixing ratio, whereas the LD band of DAPI decreases. Note, however, that an apparently rather drastic change in the magnitude of this LD band does not necessarily mean a drastic change in binding geometry as the angle is near the "magic angle" of 54.7°. The transition moment of the 350 nm band of DAPI is about 45° to the DNA helix axis: for example, increasing this angle by only 5° would result in a 50% decrease of the LD. Furthermore, as was discussed in the previous section, the decrease in LD magnitude in the DAPI absorption region couples with a corresponding decrease in DNA absorption region, suggesting that the effect is primarily due to decrease in the ability of the polynucleotide duplex to orient in the flow. Thus, both the strong positive CD and the positive LD indicate that DAPI remains minor groove-bound even in the presence of a large proportion of simultaneously bound [Ru(phen)$_2$DPPZ]$^{2+}$.

Binding Mode of [Ru(phen)$_2$DPPZ]$^{2+}$ in Minor Groove-Blocked poly[d(A−T)$_2$]. The LD spectrum of [Ru(phen)$_2$DPPZ]$^{2+}$ bound to DNA is well understood: the conspicuous difference between the LD spectra of the Δ- and Λ-enantiomers is due to a slight deviation from an idealized intercalation geometry, characterized by a clockwise roll around the complex 2-fold axis by about 10° for both enantiomers.[38,39] The magnitude and sign of the LD signal of DPPZ ligand absorption region observed in this work in the presence of DAPI, together with the strong hypochromicity, are similar to previously reported results[38,39] and confirm that the DPPZ ligand be intercalated under our conditions. For the Λ-enantiomer, the CD and LD results both suggest that the binding geometry is practically the same whether DAPI is present in the minor groove or not. For the Δ-enantiomer, the results suggest that it still binds by intercalation of the DPPZ ligand, but with a somewhat modified roll angle as a result of the presence of DAPI.

Insertion of DPPZ of the Ru Complex: From the Minor or Major Groove? The direction of intercalation of the large ligand of the ruthenium complex is still a debated question. Our observation that spectroscopic properties, especially CD and LD, of the [Ru(phen)$_2$DPPZ]$^{2+}$−poly[d(A−T)$_2$] are essentially invariant whether the minor groove of the DNA is blocked or not by DAPI, supports that the metal complex be inserted from the major groove. It is also conclusive that the binding mode of DAPI is only a little affected by the presence of the metal complexes and that the metal complex does not replace DAPI. Barton and co-workers reported[43] that the luminescence intensity of the [Ru(phen)$_2$DPPZ]$^{2+}$ complex was decreased by adding a major groove binding reagent, Δ,α-[Rh[(*R*,*R*)-Me$_2$trien]phi]$^{3+}$, but was increased by the presence of the minor groove binder distamycin, indicating that the ruthenium complex is replaced by a major groove binding reagent. These observations support the notion that there is indeed no hindrance for the [Ru(phen)$_2$DPPZ]$^{2+}$ complex to be intercalated from the major groove.

However, there is also evidence for [Ru(phen)$_2$DPPZ]$^{2+}$ intercalation from the minor groove of DNA. With the similar idea of this work, when the major groove of the duplex is blocked by a third strand, the spectral properties of both Δ- and Λ-[Ru(phen)$_2$DPPZ]$^{2+}$ enantiomers remained very similar.[34,39] Although it could be assumed that the ruthenium complexes bind to the new major groove of the triplex by analogy with the model for duplex binding,[34] the spectral properties of the metal complex in the duplex and triplex were so similar that it was concluded that these compounds be intercalated from the minor groove where they do not interfere with the third strand.[39] Luminescence titrations and excited-state decay kinetics for [Ru(phen)$_2$DPPZ]$^{2+}$ bound to calf thymus DNA and T4 DNA in which cytosine residues are 100% glycosylated in the major groove were essentially the same, supporting the intercalation of the complex from the minor groove,[40] although this conclusion has been later criticized.[43]

Given these results, we conclude that both Δ- and Λ-[Ru(phen)$_2$DPPZ]$^{2+}$ complexes can intercalate from the major groove when the minor groove of duplex DNA is blocked by DAPI (in this work) or distamycin,[43] and intercalate from the minor groove when the major groove of DNA is blocked by a third nucleic acid strand,[39] or when it is gluocosylated.[40] Because the [Ru(phen)$_2$DPPZ]$^{2+}$ complex, thus, can intercalate from either groove when the other is blocked, the possibility arises that in the absence of blocking, intercalation from minor or major both occurs in significant proportions.

Excitation Energy Transfer across the DNA Stem. Increase in emission intensity of the DNA-bound [Ru(phen)$_2$DPPZ]$^{2+}$

complex upon increasing distamycin concentration, which was particularly pronounced for poly[d(A−T)$_2$], has been reported.[43] This increase was attributed to a stiffening of the duplex DNA due to the binding of distamycin. A larger increase for poly[d(A−T)$_2$] compared to poly[d(G−C)$_2$] was ascribed to a smaller binding constant of distamycin to the latter polynucleotide.

In this work, we observed a similar increase in emission intensity of the DNA-bound [Ru(phen)$_2$DPPZ]$^{2+}$ upon addition of DAPI. This increase saturates at a stoichiometry of ∼1 DAPI/6 bp (Figure 7b). Furthermore, a decreased DAPI emission intensity upon adding [Ru(phen)$_2$DPPZ]$^{2+}$ complex was also observed (Figure 7a). It was ensured that the [Ru(phen)$_2$DPPZ]$^{2+}$ molecule neither forms any nonfluorescent complex with DAPI nor exhibits dynamic quenching activity in the absence of poly[d(A−T)$_2$]: the emission intensity of DAPI remained the same in the presence as in the absence of [Ru(phen)$_2$DPPZ]$^{2+}$. These observations ensure that the presence of poly[d(A−T)$_2$] is a prerequisite for the decrease and increase, respectively, of the emission intensity of DAPI and the metal complex to occur.

The ratio of the excitation spectra of the [Ru(phen)$_2$DPPZ]$^{2+}$−poly[d(A−T)$_2$]−DAPI and the [Ru(phen)$_2$DPPZ]$^{2+}$−poly[d(A−T)$_2$] complexes, detected through the emission of the metal complex, plotted over the DAPI absorption wavelength region, has a shape similar to the poly[d(A−T)$_2$]-bound DAPI absorption spectrum (Figure 8). This indicates that excitation energy is transferred from the DAPI molecule to the metal complex chromophore. Although stiffening of the DNA as a result of drug binding in the minor groove of DNA might be attributed to the increase in emission intensity,[43] direct transfer of the excited energy of DAPI to the ruthenium complex is a more likely explanation of the virtual increase of quantum yield. It is nevertheless interesting that the [Ru(phen)$_2$DPPZ]$^{2+}$ complex intercalated from the major groove of DNA and held together by DNA with the minor groove-bound DAPI allows excited energy of DAPI be transferred across the DNA stem.

It is noteworthy that the decrease in DAPI emission and increase in [Ru(phen)$_2$DPPZ]$^{2+}$ emission are always more pronounced for the Λ-enantiomer compared to the Δ-enantiomer (Figure 7a,b). The energy transfer is also more efficient for the Λ-enantiomer than for the Δ-enantiomer. According to the Förster theory, the distance between the donor and acceptor and their relative orientation governs the efficiency of energy transfer. The distance can be assumed to be very similar for the Λ- and Δ-enantiomers as they both intercalate from the major groove. Therefore, a difference in orientations of the enantiomers is a conceivable reason for their different energy transfer efficiencies.

Conclusion

The large DPPZ ligand of both the Δ- and Λ-enantiomers of the [Ru(phen)$_2$DPPZ]$^{2+}$ complex is intercalated from the major groove of duplex DNA when the minor groove is blocked by DAPI. A marked fluorescence resonance energy transfer between minor groove-bound DAPI and major groove-bound [Ru(phen)$_2$DPPZ]$^{2+}$ is observed, with larger efficiency for the Λ-enantiomer, possibly due to favorable orientations of donor and acceptor transition moments.

Acknowledgment. This work was supported by Korea Science and Engineering Foundation (Grant no. 2002-070-C00053).

References and Notes

(1) Nordén, B.; Lincoln, P.; Åkerman, B.; Tuite, E. In *Metal Ions in Biological System*; Sigel, A., Sigel, H., Eds.; Marcel Dekker: New York 1996; pp 177−252.
(2) Barton, J. K.; Danishefsky, A. T.; Goldberg, J. M. *J. Am. Chem. Soc*. **1984**, *106*, 2172−2176.
(3) Barton, J. K. *Science* **1986**, *233*, 727−734.
(4) Härd, T.; Hirot, C.; Nordén, B. *J. Biomol. Struct. Dynam*. **1987**, *5*. 89−96.
(5) Mei, H.-Y.; Barton, J. K. *Proc. Natl. Acad. Sci. U.S.A*. **1988**, *85*, 1339−1343.
(6) Naing, K.; Takahashi, M.; Taniguchi, M.; Yamagishi, A. *J. Chem. Soc., Chem. Commun*. **1993**, 402−403.
(7) Chow, C. S.; Barton, J. K. *Methods Enzymol*. **1992**, *212*, 217−242.
(8) Feeney, M. M.; Kelly, J. M.; Tossi, A. B.; Kirsch-De Mesmaeker, A.; Lecomte, J.-P. *J. Photochem. Photobiol. B: Biol*. **1994**, *23*, 69−78.
(9) Sentagne, C,; Chambron, J.-C.; Sauvage, J.-P.; Paillous, N. *J. Photochem. Photobiol. B: Biol*. **1994**, *26*, 165−174.
(10) Bannwarth, W.; Scimit, D.; Stallard, R. L.; Hornung, C.; Knorr, R.; Müller, F. *Helv. Chim. Acta* **1988**, *71*, 2085−2099.
(11) Bannwarth, W. *Anal. Biochem*. **1989**, *181*, 216−219.
(12) Freidman, A. E.; Chambron, J.-C.; Sauvage, J.-P.; Turro, N. J.; Barton, J. K. *J. Am. Chem. Soc*. **1990**, *112*, 4960−4962.
(13) Jenkins, Y.; Barton, J. K. *J. Am. Chem. Soc*. **1992**, *114*, 8736−8738.
(14) Xu, X.-H.; Bard, A. J. J. *Am. Chem. Soc*. **1995**, *117*, 2627−2631.
(15) Barton, J. K.; Kumar, C. V.; Turro, N. J. *J. Am. Chem. Soc*. **1986**, *108*, 6391−6393.
(16) Purugganan, M. D.; Kumar, C. V.; Turro, N. J.; Barton, J. K. *Science* **1988**, *241*, 1645−1649.
(17) Kirsch-De Mesmaeker, A.; Orellana, G.; Barton, J. K.; Turro, N. J. *Photochem. Photobiol*. **1990**, *52*, 461−472.
(18) Orellana, G.; Kirsch-De Mesmaeker, A.; Barton, J. K.; Turro, N. J. *Photochem. Photobiol*. **1991**, *54*, 499−509.
(19) Lecomte, J.-P.; Kirsch-De Mesmaeker, A.; Kelly, J. M.; Tossi, A.; Görner, H. *Photochem. Photobiol*. **1992**, *55*, 681−689.
(20) Murphy, C. J.; Arkin, M. R.; Jenkins, Y.; Ghatlia, N. D.; Bossmann, S. H.; Turro, N. J.; Barton, J. K. *Science* **1993**, *262*, 1025−1029.
(21) Murphy, C. J.; Arkin, M. R.; Ghatlia, N. D.; Bossmann, S. H.; Turro, N. J.; Barton, J. K. *Proc. Natl. Acad. Sci. U.S.A*. **1994**, *91*, 5315−5319.
(22) Stemp, E. D. A.; Arkin, M. R.; Barton, J. K. *J. Am. Chem. Soc*. **1995**, *117*, 2375−2376.
(23) Arkin, M. R.; Stemp, E. D. A.; Turro, C.; Turro, N. J.; Barton, J. K. *J. Am. Chem. Soc*. **1996**, *118*, 2267−2274.
(24) Dandliker, P. J.; Nunez, M. E.; Barton, J. K. *Biochemistry* **1988**, *27*, 6491−6502.
(25) Barton, J. K. *Pure Appl. Chem*. **1998**, *70*, 873−879.
(26) Rehmann, J. P.; Barton, J. K. *Biochemistry* **1990**, *29*, 1701−1709.
(27) Haworth, I. S.; Elcock, A. H.; Freeman, J.; Rodger, A.; Richards, W. G. *J. Biomol. Struct. Dynam*. **1987**, *5*, 89−96.
(28) Eriksson, M.; Leijon, M.; Hirot, C.; Nordén, B.; Gräslund, A. *J. Am. Chem. Soc*. **1992**, *114*, 4933−4934.
(29) Eriksson, M.; Leijon, M.; Hirot, C.; Nordén, B.; Gräslund, A. *Biochemistry* **1994**, *33*, 5031−5040.
(30) Satyanarayana, S.; Dabrowiak, J. C.; Chaires, J. B. *Biochemistry* **1992**, *31*, 9319−9324.
(31) Satyanarayana, S.; Dabrowiak, J. C.; Chaires, J. B. *Biochemistry* **1992**, *32*, 2573−2584.
(32) Lincoln, P.; Nordén, B. *J. Phys. Chem*. **1998**, *102*, 9583−9594.
(33) Wilhelmsson, L. M.; Westerlund, F.; Lincoln, P.; Nordén, B. *J. Am. Chem. Soc*. **2002**, *124*, 12092−12093.
(34) Jenkins, Y.; Freidman, A. E.; Turro, N. J.; Barton, J. K. *Biochemistry* **1992**, *31*, 10809−10816.
(35) Hiort, C.; Linclon, P.; Nordén, B. *J. Am. Chem. Soc*. **1993**, *115*, 3448−3454.
(36) Dupureur, C. M.; Barton, J. K. *J. Am. Chem. Soc*. **1994**, *116*, 10286−10287.
(37) Haq, I.; Lincoln, P.; Suh, D.; Nordén, B.; Chowdhry, B. Z.; Chaires, J. B. *J. Am. Chem. Soc*. **1995**, *117*, 4788−4796.
(38) Lincoln, P.; Broo, A.; Nordén, B. *J. Am. Chem. Soc*. **1996**, *118*, 2644−2653.
(39) Choi, S.-D.; Kim, M.-S.; Kim, S. K.; Lincoln, P.; Tuite, E.; Nordén, B. *Biochemistry* **1997**, *36*, 214−223.
(40) Tuite, E.; Lincoln, P.; Nordén, B. *J. Am. Chem. Soc*. **1997**, *119*, 239−240.
(41) Greguric, A.; Greguric, I. D.; Hambley, T. W.; Aldrich-Wright, J. R.; Collins, J. G. *J. Chem. Soc., Dalton Trans*. **2002**, 849−855.
(42) Collins, J. G.; Aldrich-Wright, J. R.; Greguric, I. D.; Pellegrini, P. A. *Inorg. Chem*. **1999**, *38*, 5502−5509.

(43) Holmlin, R. E.; Stemp, E. D. A.; Barton, J. K. *Inorg. Chem*. **1998**, *37*, 29−34.
(44) Eriksson. S.; Kim, S. K.; Kubista, M.; Nordén, B. *Biochemistry* **1993**, *32*, 2987−2998.
(45) Kim, H.-K.; Kim, J.-M.; Kim, S. K.; Rodger, A.; Nordén, B. *Biochemistry* **1996**, *35*, 1187−1194.
(46) Nordén, B.; Kubista, M.; Kurucsev, T. *Q. Rev. Biophys*. **1992**, *25*, 51−170.
(47) Nordén, B.; Kurucsev, T. *J. Mol. Recognit*. **1994**, *7*, 141−156.
(48) Nordén, B.; Seth, S. *Appl. Spectrosc*. **1985**, *39*, 647−655.
(49) Le Pecq, J. B.; Paoletti, C. *J. Mol. Biol*. **1967**, *29*, 87−106.
(50) Sehlstedt, U.; Kim, S. K.; Carter, P.; Goodisman, J.; Vollano, J. F.; Nordén, B.; Dabrowiak, J. C. *Biochemistry* **1994**, *33*, 417−416.
(51) Hyun, K.-M.; Choi, S.-D.; Lee, S.; Kim, S. K. *Biochim. Biophys. Acta* **1997**, *1334*, 312−316.